Journal of Applied Mechanics and Technical Physics, Vol. 51, No. 2, pp. 249–260, 2010

HOMOTOPY ANALYSIS METHOD FOR THERMOPHORETIC PARTICLE DEPOSITION EFFECT ON MAGNETOHYDRODYNAMIC MIXED CONVECTIVE HEAT AND MASS TRANSFER PAST A POROUS WEDGE IN THE PRESENCE OF SUCTION

R. Kandasamy and I. Muhaimin

UDC 536.24

Homotopy analysis method is used to analyze the effect of thermophoretic particle deposition on magnetohydrodynamic mixed convection flow with heat and mass transfer over a porous wedge. An explicit analytical solution is obtained which is valid throughout the solution domain and is consistent with numerical results.

Key words: *magnetohydrodynamic flow, thermophoretic particle deposition, mixed convection flow.*

Introduction. Thermophoresis is a phenomenon which causes small particles to be driven away from a hot surface toward a cold one. This phenomenon has many practical applications in removing small particles from gas streams, in determining exhaust gas particle trajectories from combustion devices, and in studying the particulate material deposition on turbine blades.

Goren [1] was one of the first to study the role of thermophoresis in laminar flow of a viscous incompressible fluid. He used the classical problem of flow over a flat plate to calculate the deposition rates and showed that substantial changes in surface deposition can be obtained by increasing the difference between the surface and free stream temperature. England and Emery [2] studied the thermal radiation effect of an optically thin gray gas bounded by a stationary vertical plate. Raptis [3] investigates radiation effect on the flow of a micropolar fluid past a continuously moving plate.

In addition, the study of magnetohydrodynamic (MHD) viscous radiating flows has important industrial, technological, and geothermal applications, such as high-temperature plasmas, cooling of nuclear reactors, fluid metal fluids, MHD accelerators, and power generation systems. Mbeledogu and Ogulu [4] investigated the heat and mass transfer of unsteady MHD natural convection flow of a rotating fluid past a vertical porous flat plate in the presence of radiative heat transfer. Alam et al. [5] studied the effects of variable suction and thermophoresis on steady MHD combined free-forced convective heat and mass transfer flow over a semi-infinite permeable inclined plate in the presence of thermal radiation. Hossain and Takhar [6] analyzed the effect of radiation, using the Rosseland diffusion approximation, on mixed convection along a vertical plate with uniform free stream velocity and surface temperature. Duwairi and Damesh [7, 8], Duwairi [9], and Damesh et al. [10] studied the effect of radiation and heat transfer in different geometries for various flow conditions.

Thermophoretic deposition of radioactive particles is considered to be one of the important factors causing accidents in nuclear reactors. Goldsmith and May [11] were the first to study the thermophoretic transport involved in simple one-dimensional flow for the purpose of measuring the thermophoretic velocity. Thermophoresis in natural convection with variable properties for a laminar flow over a cold vertical flat plate was studied by Jayaraj et al. [12]. Selim et al. [13] explored the effect of surface mass flux on mixed convective flow past a heated vertical flat permeable plate with thermophoresis. The first analysis of thermophoretic deposition in geometry of engineering interest appears to be that of Hales et al. [14]. They solved the laminar-boundary-layer equations for simultaneous

University Tun Hussein Onn, Parit Raja 86400, Batu Pahat, Johor, Malaysia; future990@gmail.com. Translated from Prikladnaya Mekhanika i Tekhnicheskaya Fizika, Vol. 51, No. 2, pp. 126–139, March–April, 2010. Original article submitted May 19, 2009.

0021-8944/10/5102-0249 © 2010 Springer Science + Business Media, Inc.

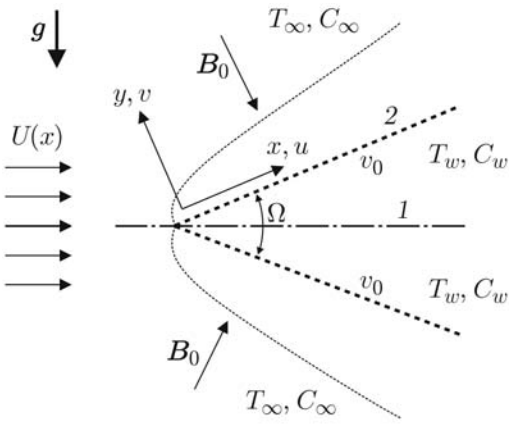

Fig. 1. Flow diagram along the wall of the wedge: 1) wedge; 2) porous wall.

aerosol and steam transport to an isothermal vertical surface situated adjacent to a large body of an otherwise quiescent air-steam-aerosol mixture. Recently, Chamkha and Pop [15] studied the effect of thermophoretic particle deposition in a free-convection boundary layer from a vertical flat plate embedded in a porous medium.

A few representative fields of interest in which combined heat and mass transfer with thermophoresis effect plays an important role are: design of chemical processing equipment, formation and dispersion of fog, distribution of temperature and moisture over agricultural fields and groves of fruit trees, damage of crops due to freezing, food processing, and cooling towers. In particular, the study of heat and mass transfer with thermophoretic particle deposition is of considerable importance for chemical and hydrometallurgical industries. Of particular importance is an understanding of combined heat and mass transfer by mixed convection from a heated flat surface embedded in a fluid-saturated porous medium [16]. Numerical results of solution of this problem were reported by Murthy and Singh [17]. However, to our knowledge, no one has reported an analytical solution for this problem. In this paper, we employ the homotopy analysis method (HAM) [18–23] to give such an explicit analytical solution.

1. Mathematical Model. We consider a wedge plate embedded in a saturated porous medium as shown in Fig. 1. In Fig. 1, v_0 is the velocity of suction if $v_0 < 0$ and is the velocity of injection if $v_0 > 0$. The plate may be permeable ($v_w \neq 0$) or impermeable ($v_w = 0$). The surface of the plate is maintained at a constant temperature T_w higher than the ambient temperature T_∞, and, at the same time, the concentration of a constituent decreases from C_w at the wall to C_∞ sufficiently away from the wall. Let the x axis be taken along the direction of the wedge, and the y axis normal to it. Fluid suction or injection is imposed at the wedge surface (see Fig. 1). The temperature gradient in the y direction is much higher than that in the x direction, and hence only the thermophoretic velocity component which is normal to the surface is of importance. Invoking the Boussinesq and boundary-layer approximations, we write the governing equations based on the Forchheimer formulation as

$$\frac{\partial u}{\partial x} + \frac{\partial v}{\partial y} = 0; \tag{1}$$

$$u\,\frac{\partial u}{\partial x} + v\,\frac{\partial u}{\partial y} = \nu\,\frac{\partial^2 u}{\partial y^2} + U\,\frac{dU}{dx} - \Big(\frac{\sigma B_0^2}{\rho} + \frac{\nu}{K}\Big)(u - U) - \frac{\mathrm{F}}{\sqrt{K}}\,(u^2 - U^2)$$

$$+ [g\beta(T - T_\infty) + g\beta^*(C - C_\infty)]\sin\frac{\Omega}{2}; \tag{2}$$

$$u\,\frac{\partial T}{\partial x} + v\,\frac{\partial T}{\partial y} = \alpha\,\frac{\partial^2 T}{\partial y^2}, \qquad u\,\frac{\partial C}{\partial x} + v\,\frac{\partial C}{\partial y} = D\,\frac{\partial^2 C}{\partial y^2} - \frac{\partial\,(V_T C)}{\partial y}. \tag{3}$$

The boundary conditions are

$$u = 0, \quad v = v_w, \quad T = T_w, \quad C = C_w \quad \text{at} \quad y = 0,$$

$$u = U(x), \quad T = T_\infty, \quad C = C_\infty \quad \text{at} \quad y \to \infty.$$

Here u and v are the velocity components in the x and y directions, respectively, ν is the kinematic viscosity, g is the acceleration due to gravity, ρ is the density of the fluid, β is the thermal-expansion coefficient, β^* is the volumetric-expansion coefficient, T, T_w, and T_∞ are the temperature of the fluid in the thermal boundary layer, the plate temperature, and the fluid temperature in the free stream, respectively, C, C_w, and C_∞ are the corresponding concentrations, α is the thermal conductivity of the fluid, D is the effective diffusion coefficient, $\boldsymbol{B}_0$ is the constant magnetic field strength, σ is the electric conductivity, K is the permeability of the porous medium, Ω is the angle of inclination of the wedge, $V_T = -(k\nu/T)\,\partial T/\partial y$ is the thermophoretic velocity, k is the thermophoretic coefficient, and F is an empirical constant (Forchheimer number). The third and fourth terms on the right side of Eq. (2) represent the resistance proportional to the first power of the velocity (Darcy law) and the resistance proportional to the second power of the velocity (porous inertia), respectively. For $\mathrm{F} = 0$, the expression for the force of resistance reduces to the Darcy law.

Following [24], we make the change of variables

$$\eta(x,y) = y\sqrt{\frac{(1+m)U}{2\nu x}}, \qquad \psi(x,y) = \sqrt{\frac{2U\nu\,x}{1+m}}\,f(x,\eta).$$

The potential-flow velocity can be expressed as

$$U(x) = Ax^m, \qquad \beta_1 = 2m/(1+m),$$

where A is a constant and $\beta_1 = \Omega/\pi$ is the Hartree pressure gradient parameter.

The continuity equation (1) implies the existence of the stream function $\psi(x,y)$

$$u = \frac{\partial\psi}{\partial y}, \qquad v = -\frac{\partial\psi}{\partial x}.$$

Let us transform Eqs. (2) and (3) to a system of ordinary differential equations. For this, we introduce the following dimensionless parameters and variables: θ is the temperature, φ is the concentration, Gr is the Grashof number, Ec is the Eckert number, N is the buoyancy ratio, Re_x is the Reynolds number, Re_k is the local Reynolds number, Pr is the Prandtl number, M_* is the magnetic parameter, Fn is the Forchheimer number, Sc is the Schmidt number, S is the injection or suction parameter, λ is the porosity parameter of the medium, and τ is the thermophoretic parameter:

$$\theta = \frac{T-T_\infty}{T_w-T_\infty}, \quad \varphi = \frac{C-C_\infty}{C_w-C_\infty}, \quad \mathrm{Gr} = \frac{\nu g\beta(T-T_\infty)}{U^3}, \quad \mathrm{Ec} = \frac{c^2}{c_p(T_w-T_\infty)}\,(k^2)^{2m/(1-m)},$$

$$N = \frac{\beta^*(C_w-C_\infty)}{\beta(T_w-T_\infty)}, \quad \mathrm{Re}_x = \frac{Ux}{\nu}, \quad \mathrm{Re}_k = \frac{U\sqrt{K}}{\nu}, \quad \mathrm{Pr} = \frac{\nu}{\alpha}, \quad M_* = \frac{\sigma B_0^2}{\rho a}, \tag{4}$$

$$\mathrm{Fn} = \frac{\mathrm{F}\,U\sqrt{K}}{\nu}, \quad \mathrm{Sc} = \frac{\nu}{D}, \quad S = f_w = -v_w\sqrt{\frac{(1+m)x}{2\nu U}}, \quad \lambda = \frac{\alpha}{KU}, \quad \tau = -\frac{k(T_w-T_\infty)}{T_r}$$

(c_p is the heat capacity at constant pressure). Equations (2) and (3) become

$$\frac{\partial^3 f}{\partial\eta^3} = -f\,\frac{\partial^2 f}{\partial\eta^2} - \frac{2m}{1+m}\Big(1-\Big(\frac{\partial f}{\partial\eta}\Big)^2\Big) - \frac{2(N\varphi+\theta)}{1+m}\,\mathrm{Gr}\,\mathrm{Re}_x\sin\frac{\Omega}{2}$$

$$+\,\frac{2x}{1+m}\Big(\frac{\partial f}{\partial\eta}\,\frac{\partial^2 f}{\partial x\,\partial\eta} - \frac{\partial f}{\partial x}\,\frac{\partial^2 f}{\partial\eta^2}\Big) + \frac{2}{m+1}\,(M_*+\lambda)\Big(\frac{\partial f}{\partial\eta}-1\Big) + \frac{2}{m+1}\,\frac{\mathrm{F}\,x}{\sqrt{K}}\Big(\Big(\frac{\partial f}{\partial\eta}\Big)^2-1\Big),$$

$$\frac{\partial^2\theta}{\partial\eta^2} = -\mathrm{Pr}\,\frac{\partial\theta}{\partial\eta} + \frac{2\mathrm{Pr}}{1+m}\,\theta\,\frac{\partial f}{\partial\eta} + \mathrm{Pr}\,\frac{2x}{1+m}\Big(\frac{\partial f}{\partial\eta}\,\frac{\partial\theta}{\partial x} - \frac{\partial f}{\partial x}\,\frac{\partial\theta}{\partial\eta}\Big), \tag{5}$$

$$\frac{\partial^2\varphi}{\partial\eta^2} = -\,\mathrm{Sc}\Big(f-\tau\,\frac{\partial\theta}{\partial\eta}\Big)\frac{\partial\varphi}{\partial\eta} + \frac{2\,\mathrm{Sc}}{1+m}\,\varphi\,\frac{\partial f}{\partial\eta} + \frac{2x\,\mathrm{Sc}}{1+m}\Big(\frac{\partial f}{\partial\eta}\,\frac{\partial\varphi}{\partial x} - \frac{\partial f}{\partial x}\,\frac{\partial\varphi}{\partial\eta}\Big) + \mathrm{Sc}\,\tau\,\frac{\partial^2\theta}{\partial\eta^2}\,\varphi.$$

The boundary conditions are written as

$$\begin{aligned}
&\eta = 0: \qquad \frac{\partial f}{\partial \eta} = 0, \quad \frac{f}{2}\Big(1 + \frac{x}{U}\,\frac{dU}{dx}\Big) + x\,\frac{\partial f}{\partial x} = -v_0\sqrt{\frac{(1+m)x}{2\nu U}}, \quad \theta = 1, \quad \varphi = 1,\\
&\eta \to \infty: \qquad \frac{\partial f}{\partial \eta} = 1, \quad \theta = 0, \quad \varphi = 0.
\end{aligned} \tag{6}$$

Equations (5) with boundary conditions (6) can be represented as

$$\begin{aligned}
&\frac{\partial^3 f}{\partial \eta^3} + \Big(f + \frac{1-m}{1+m}\,\xi\,\frac{\partial f}{\partial \xi}\Big)\frac{\partial^2 f}{\partial \eta^2} - \frac{1-m}{1+m}\,\xi\,\frac{\partial^2 f}{\partial \xi\,\partial \eta}\,\frac{\partial f}{\partial \eta} + \frac{2(N\varphi+\theta)}{1+m}\,\mathrm{Gr}\,\mathrm{Re}_x \sin\frac{\Omega}{2}\\
&- \frac{2}{m+1}\,\xi^2(M_* + \lambda)\Big(\frac{\partial f}{\partial \eta} - 1\Big) - \frac{2}{m+1}\Big(\Big(\frac{\partial f}{\partial \eta}\Big)^2 - 1\Big)\Big(\frac{\mathrm{Re}_x}{(\mathrm{Re}_k)^2}\ \mathrm{Fn} + m\Big) = 0,\\
&\frac{\partial^2 \theta}{\partial \eta^2} + \mathrm{Pr}\,\Big(f + \frac{1-m}{1+m}\,\xi\,\frac{\partial f}{\partial \xi}\Big)\frac{\partial \theta}{\partial \eta} - \frac{2\mathrm{Pr}}{1+m}\,\theta\,\frac{\partial f}{\partial \eta} - \frac{1-m}{1+m}\,\xi\,\frac{\partial \theta}{\partial \xi}\,\frac{\partial f}{\partial \eta} = 0,\\
&\frac{\partial^2 \varphi}{\partial \eta^2} + \mathrm{Sc}\,\Big(f - \tau\,\frac{\partial \theta}{\partial \eta}\Big)\frac{\partial \varphi}{\partial \eta} + \mathrm{Sc}\ \frac{1+m}{1-m}\Big(\frac{\partial \varphi}{\partial \eta}\,\xi\,\frac{\partial f}{\partial \xi} - \frac{\partial f}{\partial \eta}\,\xi\,\frac{\partial \varphi}{\partial \xi}\Big)\\
&- \frac{2\,\mathrm{Sc}}{1+m}\,\varphi\,\frac{\partial f}{\partial \eta} - \mathrm{Sc}\,\tau\,\frac{\partial^2 \theta}{\partial \eta^2}\,\varphi = 0;\\
&\eta = 0: \qquad \frac{\partial f}{\partial \eta} = 0, \quad \frac{(1+m)f}{2} + \frac{1-m}{2}\,\xi\,\frac{\partial f}{\partial \xi} = f_w, \quad \theta = 1, \quad \varphi = 1,\\
&\eta \to \infty: \qquad \frac{\partial f}{\partial \eta} = 1, \quad \theta = 0, \quad \varphi = 0.
\end{aligned} \tag{7}$$

Here $f_w = S$ is the suction parameter if $f_w > 0$ and injection parameter if $f_w < 0$, Fn is the dimensionless inertial parameter (Forchheimer number), $\xi = kx^{(1-m)/2} > 0$ is the dimensionless distance along the wedge [24], and $f(\xi, \eta)$ is the dimensionless stream function. Obviously, if all terms with derivatives with respect to ξ are retained, it is necessary to employ a numerical scheme suitable for partial differential equations for the solution of the problem. In addition, because the streamwise solution depends on the derivatives with respect to ξ, a locally autonomous solution cannot be obtained at an arbitrary specified point along the point. In this case, an implicit marching numerical solution scheme is usually applied before the solution in the ξ direction, i.e., the solution is calculated at the point ξ_{i+1} when it is known at the point ξ_i. However, when the terms containing the derivatives $\partial f/\partial \xi$, $\partial \theta/\partial \xi$, and $\partial \varphi/\partial \xi$ and their derivatives with respect to η are absent, the system of ordinary differential equations for the functions f, θ, and φ with the parameter ξ takes place, and the procedure of its solution is simplified. Furthermore, a locally autonomous solution can be obtained for any ξ. According to [24, 25], in the present numerical solution of the problem, the shooting method is used. By virtue of the aforesaid, for $\xi = 1$, Eqs. (7) are transformed to the equations

$$\begin{aligned}
&f''' + ff'' + \frac{2}{1+m}\,(1 - f'^2)\Big(\frac{\mathrm{Re}_x}{(\mathrm{Re}_k)^2}\ \mathrm{Fn} + m\Big) + \frac{2(N\varphi+\theta)}{1+m}\,\mathrm{Gr}\,\mathrm{Re}_x \sin\frac{\Omega}{2} - \frac{2}{1+m}\,(M_* + \lambda)(f' - 1) = 0,\\
&\theta'' + \mathrm{Pr}\,f\theta' - \frac{2\mathrm{Pr}}{1+m}\,\theta f' = 0,\\
&\varphi'' + \mathrm{Sc}(f - \tau\theta')\varphi' - \frac{2\,\mathrm{Sc}}{1+m}\,f'\varphi - \mathrm{Sc}\,\tau\theta''\varphi = 0
\end{aligned} \tag{8}$$

with the boundary conditions

$$\begin{aligned}
&\eta = 0: \qquad f = 2f_w/(1+m), \quad f' = 0, \quad \theta = 1, \quad \varphi = 1,\\
&\eta \to \infty: \qquad f' = 1, \quad \theta = 0, \quad \varphi = 0.
\end{aligned} \tag{9}$$

2. Numerical Solution. The system of nonlinear ordinary differential equations (8) with boundary conditions (9) was solved by using the Gill method [25] and the shooting technique with prescribed parameters α, Ω, λ, M_*, and τ. The computation was made with Matlab software. In most cases, a step size $\Delta\eta = 0.001$ was selected to satisfy a convergence criterion of 10^{-7}. The maximum value of η_∞ for each set of the parameters α, Ω, γ, and τ was determined so that, in the case of a successful iteration, the values of the unknowns on the boundary $\eta = 0$ changed with an error less than 10^{-7}. The thermophoretic particle deposition in magnetohydrodynamic (MHD) mixed convective heat and mass transfer over a porous wedge was studied for various values of suction at the wall of the wedge.

3. Analytical Solution. The functions $f(\eta)$, $\theta(\eta)$, and $\varphi(\eta)$ can be expressed from the boundary conditions (9) as follows:

$$f(\eta) = \sum_{n=0}^{+\infty} A_n \exp(-n\gamma\eta), \qquad \theta(\eta) = \sum_{n=1}^{+\infty} B_n \exp(-n\gamma\eta), \qquad \varphi(\eta) = \sum_{n=1}^{+\infty} C_n \exp(-n\gamma\eta).$$

Here A_n, B_n, and C_n are coefficients to be determined and $\gamma > 0$ is a constant. As the initial approximation, from (9) it is straightforward to choose the functions

$$\begin{gathered} f_0(\eta) = 1 + f_w - \exp(-\gamma\eta), \\ \theta_0(\eta) = \frac{\exp(-\gamma\eta) + \exp(-2\gamma\eta)}{2}, \qquad \varphi_0(\eta) = \frac{\exp(-\gamma\eta) + \exp(-2\gamma\eta)}{2}. \end{gathered} \tag{10}$$

In addition, we define the auxiliary linear operators

$$L_1 = \frac{\partial}{\partial\eta}\Big(\frac{\partial^2}{\partial\eta^2} - 1\Big), \qquad L_2 = \exp(\gamma\eta)\Big(\frac{\partial^2}{\partial\eta^2} - 1\Big)$$

with the following properties:

$$L_1(C_1 + C_2\exp(\eta) + C_3\exp(-\eta)) = 0, \qquad L_2(C_4(\exp(-\eta) + C_5\exp(\eta)) = 0$$

($C_1, C_2, \ldots, C_5$ are constants of integration).

Next, we construct the so-called zero-order deformation equations

$$(1-p)L_1[\mathrm{F}(\eta;P) - f_0(\eta)] = ph_f N_f[\mathrm{F}(\eta;p), \theta(\eta;p), \varphi(\eta;p)],$$

$$(1-p)L_2[\theta(\eta;P) - \theta_0(\eta)] = ph_\theta N_\theta[\mathrm{F}(\eta;p), \theta(\eta;p)],$$

$$(1-p)L_3[\varphi(\eta;P) - \varphi_0(\eta)] = ph_\varphi N_\varphi[\mathrm{F}(\eta;p), \varphi(\eta;p)]$$

with the boundary conditions

$$\mathrm{F}(0;p) = f_w, \qquad \frac{\partial\,\mathrm{F}(\eta;p)}{\partial\eta}\Big|_{\eta=0} = 0, \qquad \theta(0;p) = \varphi(0;p) = 1,$$

$$\frac{\partial\,\mathrm{F}(\eta;p)}{\partial\eta}\Big|_{\eta=\infty} = 1, \qquad \theta(0;p) = \varphi(0;p) = 0.$$

Here

$$\begin{aligned} N_f[\mathrm{F},\theta,\varphi] &= \frac{\partial^3\mathrm{F}}{\partial\eta^3} + \mathrm{F}\ \frac{\partial^2\mathrm{F}}{\partial\eta^2} + \frac{2}{1+m}\Big(1 - \Big(\frac{\partial\,\mathrm{F}}{\partial\eta}\Big)^2\Big)\Big(\frac{\mathrm{Re}_x}{(\mathrm{Re}_k)^2}\ \mathrm{Fn} + m\Big) \\ &+ \frac{2(N\varphi+\theta)}{1+m}\mathrm{Gr}\,\mathrm{Re}_x\sin\frac{\Omega}{2} - \frac{2}{1+m}\,(M_* + \lambda)\Big(\frac{\partial\,\mathrm{F}}{\partial\eta} - 1\Big), \\ N_\theta[\mathrm{F};\theta] &= \frac{\partial^2\theta}{\partial\eta^2} + \mathrm{Pr}\ \mathrm{F}\ \frac{\partial\theta}{\partial\eta} - \frac{2\mathrm{Pr}}{1+m}\,\theta\,\frac{\partial\,\mathrm{F}}{\partial\eta}, \\ N_\varphi[\mathrm{F};\varphi] &= \frac{\partial^2\varphi}{\partial\eta^2} + \mathrm{Sc}\ \Big(\mathrm{F} - \tau\,\frac{\partial\theta}{\partial\eta}\Big)\,\frac{\partial\varphi}{\partial\eta} - \frac{2\,\mathrm{Sc}}{1+m}\,\frac{\partial\,\mathrm{F}}{\partial\eta}\,\varphi - \mathrm{Sc}\,\tau\,\frac{\partial^2\theta}{\partial\eta^2}\,\varphi, \end{aligned} \tag{11}$$

$p \in [0,1]$ is the embedding parameter and h_f, h_θ, and h_φ are auxiliary nonzero parameters. Obviously,

$$\mathrm{F}(\eta;0)=f_0(\eta),\quad \mathrm{F}'(\eta;0)=f_0'(\eta),\quad \theta(\eta;0)=\theta_0(\eta),\quad \varphi_0(\eta;0)=\varphi_0(\eta)\quad \text{at}\quad p=0,$$
$$\mathrm{F}'(\eta;1)=f'(\eta),\quad \theta(\eta;1)=\theta(\eta),\quad \varphi(\eta;1)=\varphi(\eta)\quad \text{at}\quad p=1. \tag{12}$$

We expand the functions $\mathrm{F}(\eta;p)$, $\theta(\eta;p)$, and $\varphi(\eta;p)$ in a Taylor power series at the point $p=0$:

$$\mathrm{F}(\eta;p)=\mathrm{F}(\eta;0)+\sum_{l=1}^{+\infty}f_l(\eta)p^l,\qquad \theta(\eta;p)=\theta(\eta;0)+\sum_{l=1}^{+\infty}\theta_l(\eta)p^l,$$
$$\varphi(\eta;p)=\varphi(\eta;0)+\sum_{l=1}^{+\infty}\varphi_l(\eta)p^l. \tag{13}$$

Here

$$f_l(\eta)=\frac{1}{l!}\,\frac{\partial^l\mathrm{F}(\eta;p)}{\partial p^l}\Big|_{p=0},\qquad \theta_l(\eta)=\frac{1}{l!}\,\frac{\partial^l\theta(\eta;p)}{\partial p^l}\Big|_{p=0},\qquad \varphi_l(\eta)=\frac{1}{l!}\,\frac{\partial^l\varphi(\eta;p)}{\partial p^l}\Big|_{p=0}.$$

We note that the convergence regions of series (13) depend on the auxiliary parameters h_f, h_θ, and h_φ. If the parameters h_f, h_θ, and h_φ are chosen so that series (13) converge for $p=1$, in view of (12), we have

$$f(\eta)=f_0(\eta)+\sum_{l=1}^{+\infty}f_l(\eta),\qquad \theta(\eta)=\theta_0(\eta)+\sum_{l=1}^{+\infty}\theta_l(\eta),\qquad \varphi(\eta)=\varphi_0(\eta)+\sum_{l=1}^{+\infty}\varphi_l(\eta). \tag{14}$$

Differentiating Eqs. (11) m times with respect p, then setting $p=0$, and finally dividing these equations by $m!$, we obtain the so-called mth-order equations for f_l, θ_l, and φ_l (for details, see [22, 23])

$$L_f[f_l(\eta)-\chi_l f_{l-1}(\eta)]=h_f R_l(\eta),\qquad L_\theta[\theta_l(\eta)-\chi_l\theta_{l-1}(\eta)]=h_\theta S_l(\eta),$$
$$L_\varphi[\varphi_l(\eta)-\chi_l\varphi_{l-1}(\eta)]=h_\varphi W_l(\eta) \tag{15}$$

with the boundary conditions

$$f_l(0)=f_w,\quad f_l'(0)=0,\quad \theta_l(0)=\varphi_l(0)=0,\quad f_l'(\infty)=1,\quad \theta_l(\infty)=\varphi_l(\infty)=0. \tag{16}$$

Here

$$R_l(\eta)=f_{l-1}'''(\eta)+\frac{2}{1+m}\Big(\frac{\mathrm{Re}_x}{(\mathrm{Re}_k)^2}\ \mathrm{Fn}\ +m\Big)-\frac{2}{1+m}\Big(\frac{\mathrm{Re}_x}{(\mathrm{Re}_k)^2}\,\mathrm{Fn}\ +m\Big)\sum_{n=0}^{l-1}f_n'(\eta)f_{l-1-n}'(\eta)$$
$$+\frac{2}{1+m}\,(M_*+\lambda)+\frac{2(N\varphi_{l-1}(\eta)+\theta_{l-1}(\eta))}{1+m}\,\mathrm{Gr}\,\mathrm{Re}_x\sin\frac{\Omega}{2}$$
$$-\frac{2}{1+m}\,(M_*+\lambda)\sum_{n=0}^{l-1}f_{l-1-n}'(\eta)+\sum_{n=0}^{l-1}f_n(\eta)f_{l-1-n}''(\eta),$$

$$S_l(\eta)=\theta_{l-1}''(\eta)+\mathrm{Pr}\sum_{n=0}^{l-1}\Big[f_n(\eta)\theta_{l-1-n}'(\eta)-\frac{2}{1+m}\,\theta_{l-1-n}(\eta)f_n'(\eta)\Big],$$

$$W_l(\eta)=\varphi_{l-1}''(\eta)-\mathrm{Sc}\sum_{n=0}^{l-1}\Big[\frac{2}{1+m}\,\varphi_{l-1-n}(\eta)f_n'(\eta)-\tau\varphi_{l-1-n}(\eta)\theta_n''(\eta)\Big]+\mathrm{Sc}\sum_{n=0}^{l-1}(f_n(\eta)-\tau\theta_n'(\eta))\varphi_{l-1-n}'(\eta),$$

$$\chi_l=\begin{cases}0, & l\leqslant 1,\\ 1, & l>1.\end{cases}$$

The functions f_l, θ_l, and φ_l which satisfy (15) and (16) have the form

$$f_l(\eta)=\sum_{l=1}^{2l+1}a_{l,k}\exp(-k\gamma\eta),\qquad \theta_l(\eta)=\sum_{k=1}^{2l+2}b_{l,k}\exp(-k\gamma\eta),\qquad \varphi_l(\eta)=\sum_{k=1}^{2l+2}c_{l,k}\exp(-k\gamma\eta)\quad \text{at}\quad m\geqslant 1,$$

where $a_{l,k}$, $b_{l,k}$, and $c_{l,k}$ are coefficients. Substituting these expressions into (15) and (16), we obtain the recursive formulas

$$a_{l,k} = \frac{h_f}{k(k^2-1)\gamma^3}\,\Gamma_{l,k} + \chi_l \lambda_{l-1,k+2} a_{l-1,k}, \quad 1 \leqslant k \leqslant 2l+1, \qquad a_{l,0} = -\sum_{k=1}^{2l+1} a_{l,k},$$

$$b_{l,k} = \frac{h_\theta}{(k^2-1)\gamma^2}\,\Lambda_{l,k-1} + \chi_l \lambda_{l-1,k} b_{l-1,k}, \quad 2 \leqslant k \leqslant 2l+2, \qquad b_{l,1} = -\sum_{k=2}^{2l+2} b_{l,k},$$

$$c_{l,k} = \frac{h_\varphi}{(k^2-1)\gamma^2}\,\Delta_{l,k-1} + \chi_l \lambda_{l-1,k} c_{l-1,k}, \quad 2 \leqslant k \leqslant 2l+2, \qquad c_{l,1} = -\sum_{k=2}^{2l+2} c_{l,k}.$$

Here

$$\Gamma_{l,k} = \lambda_{l-1,k+2} a_{l-1,k+2} (k\gamma)^3 + (N c_{l-1,k} + b_{l-1,k}) \mathrm{Gr}\,\mathrm{Re}_x\, \sin\frac{\Omega}{2}\,(k\gamma) + \frac{2}{1+m}\Big(\frac{\mathrm{Re}_x}{(\mathrm{Re}_k)^2}\,\mathrm{Fn} + m\Big) + \frac{2}{1+m}\,(M_* + \lambda) + \beta_{l,k},$$

$$\Lambda_{l,k} = \lambda_{l-1,k+1} a_{l-1,k} (k\gamma)^2 + \theta_{l,k}, \qquad 1 \leqslant k \leqslant 2l+1,$$

$$\Delta_{l,k} = \lambda_{l-1,k+1} a_{l-1,k} (k\gamma)^2 + \varphi_{l,k}, \qquad 1 \leqslant k \leqslant 2l+1.$$

By the definitions,

$$\beta_{l,k} = \sum_{n=0}^{l-1} \sum_{s=\max(1,k-2n-1)}^{\min(2l-2n,k)} \Bigg[(s-k) s^2 \gamma^3 \frac{2}{1+m} b_{n,k-s} a_{l-1-n,s}$$

$$- (s-k) s \gamma^2 \frac{2}{1+m}\, a_{n,k-s} a_{l-1-n,s} - \frac{2}{1+m}\Big(\frac{\mathrm{Re}_x}{(\mathrm{Re}_k)^2}\,\mathrm{Fn} + m\Big) s^2 \gamma^2 a_{n,k-s} a_{l-1-n,s}$$

$$- \frac{2}{1+m}\,(M_* + \lambda) s \gamma a_{l-i-n,s} \Bigg], \quad 2 \leqslant k \leqslant 2l+2, \qquad \beta_{l,1} = 0, \qquad \beta_{l,2l+1} = 0,$$

$$\theta_{l,k} = \mathrm{Pr} \sum_{n=0}^{m-1} \sum_{s=\max(1,k-2n-1)}^{\min(2l-2n,k)} \Big[\gamma s a_{n,k-s} b_{l-1-n,s} - \frac{2}{1+m}\, a_{n,k-s} b_{l-1-n,s} \Big], \qquad 1 \leqslant k \leqslant 2l+1,$$

$$\varphi_{l,k} = \mathrm{Sc} \sum_{n=0}^{m-1} \sum_{s=\max(1,k-2n-1)}^{\min(2l-2n,k)} \Big[- \frac{2}{1+m}\, a_{n,k-s} c_{l-1-n,s} - \frac{2}{1+m}\, \tau b_{n,k-s} c_{l-1-n,s}$$

$$+ \gamma s (a_{n,k-s} - \tau b_{n,k-s}) c_{l-1-n,s} \Big], \qquad 1 \leqslant k \leqslant 2l+1,$$

$$\lambda_{l,k} = \begin{cases} 1, & 1 \leqslant k \leqslant 2l+2, \\ 0, & k < 1, \quad k > 2l+2. \end{cases}$$

Using the above recursive formulas, we can calculate all coefficients of approximation (10):

$$a_{0,0} = 1 + f_w, \qquad a_{0,1} = -1, \qquad b_{0,1} = b_{0,2} = c_{0,1} = c_{0,2} = 1/2.$$

The corresponding approximations (14) of the Mth order are given by

$$f(\eta) = f_0(\eta) + \sum_{l=1}^{M} f_l(\eta) = \sum_{l=0}^{M} \sum_{k=0}^{2l+1} a_{l,k} \exp(-k\gamma\eta),$$

$$\theta(\eta) = \theta_0(\eta) + \sum_{l=1}^{M} \theta_l(\eta) = \sum_{l=0}^{M} \sum_{k=1}^{2l+2} b_{l,k} \exp(-k\gamma\eta), \qquad \varphi(\eta) = \varphi_0(\eta) + \sum_{l=1}^{M} \varphi_l(\eta) = \sum_{l=0}^{M} \sum_{k=1}^{2l+2} c_{l,k} \exp(-k\gamma\eta);$$

for $M \to +\infty$, they represent the analytical solution (8).

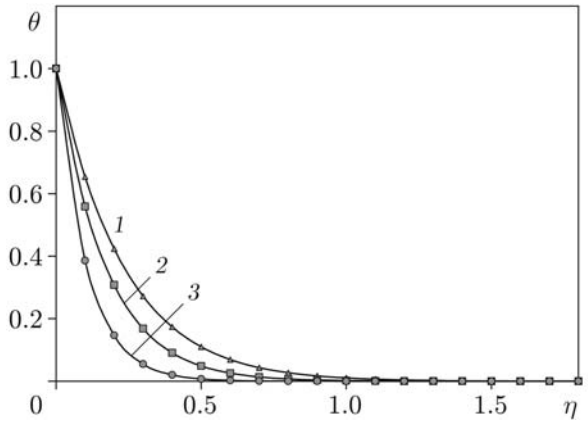

Fig. 2

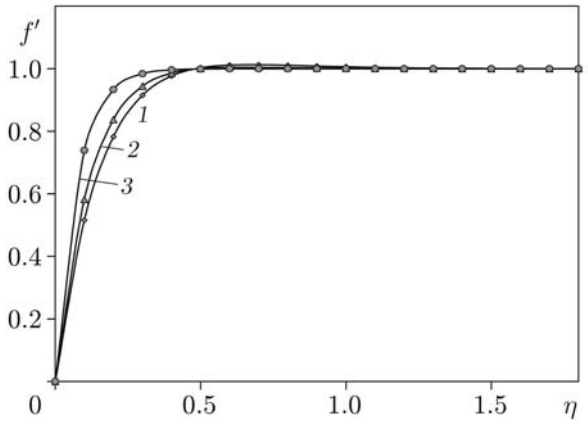

Fig. 3

Fig. 2. Temperature versus variable η for $\mathrm{Re}_x = 3$, $\mathrm{Re}_k = 1$, $\mathrm{Gr} = \mathrm{Fn} = M_* = N = 1$, $\mathrm{Sc} = 0.62$, $S = 1$, $\gamma = 1$, $M = 80$, $\tau = 1$, and $\mathrm{Pr} = 0.3$ (1), 0.73 (2), and 3 (3); points correspond to numerical calculation results, and curves to the analytical solution.

Fig. 3. Velocity versus variable η for $\mathrm{Re}_x = 3$, $\mathrm{Re}_k = \mathrm{Gr} = \mathrm{Fn} = M_* = N = 1$, $\mathrm{Sc} = 0.62$, $\mathrm{Pr} = 0.73$, $\gamma = 1$, $M = 80$, $\tau = 1$, and $S = 3$ (1), 5 (2), and 8 (3); points refer to numerical calculation results and curves to the analytical solution.

4. Validation of the Analytical Solution. In this section, we verify our analytical solutions by numerical integration using the fourth-order Runge–Kutta method and Newton–Raphson technique. As the initial approximation of the numerical solutions we use the values of the functions f_0, θ_0, and φ_0 defined by Eqs. (10). To satisfy the boundary conditions at infinity, the integration distance η_∞ was chosen equal 40 and was discretized into 10,000 intervals. The iterative integration procedure was repeated until the root-mean-square error for each discretized Eq. (8) reached not more than $5 \cdot 10^{-6}$.

We note that our explicit analytical solution contains the free parameters h_f, h_θ, h_φ, and γ which provides convergence of series (14) (see [18–23]). The parameters used for the analytical solution are listed in Table 1 ($\mathrm{Re}_x = 3$, $\tau = 1$, $\mathrm{Pr} = 0.71$, and $\mathrm{Sc} = 0.62$). Tables 2–4 gives analytical solutions of various orders of approximation and numerical calculation results for $\mathrm{Re}_x = 3$, $\mathrm{Re}_k = 1$, $\mathrm{Gr} = 1$, $\mathrm{Fn} = 1$, $N = 1$, $\mathrm{Pr} = 0.73$, $\mathrm{Sc} = 0.62$, $f_w = 1$, and $M_* = \tau = 1$. From Tables 2–4, it follows that our analytical approximations agree well with the numerical ones as long as the order of approximation is high enough.

The velocity, temperature, and concentration profiles obtained in the dimensionless form η are presented in Figs. 2–5 for $\mathrm{Pr} = 0.73$, which corresponds to air at a temperature 20°C, and $\mathrm{Sc} = 0.62$, which corresponds to water vapor. These values of Pr and Sc are of great interest for studies of diffusion of chemical impurity in air. The following parameter values of the model were chosen: Grashof number $\mathrm{Gr} = 1$ (for $\mathrm{Gr} > 0$ cooling), Eckert number $\mathrm{Ec} = 0.001$, buoyancy ratio $N = 1$, local Reynolds number $\mathrm{Re}_k = 1$, $m = 0.0909$ (for an angle of inclination of the wedge $\Omega = 30°$), porosity parameter of the medium $\lambda = 1$, and Reynolds number $\mathrm{Re}_x = 3$. From Figs. 2–5, it follows that the analytical solutions are in good agreement with the numerical calculation results.

5. Discussion of Results. The analytical solutions presented in Fig. 2 agree well with the numerical calculation results and data given by Watanabe and Morioka [25]. It should be pointed out that Watanabe and Morioka presented numerical results for the Prandtl number Pr in the range of 0.3–15.0. However, for $\mathrm{Pr} > 7$, a higher order of approximation is needed. Because of limited capacity of our computer, we were unable to give sufficiently accurate analytical solutions for $\mathrm{Pr} > 7$, although our analytical solution is valid for any combination of Re_x, Gr, Fn, N, Sc, f_w, and τ if the parameters h_f, h_θ, h_φ, and γ are properly selected and the order of approximation is high enough. Even though, our analytical solution agree well with numerical results for a wide range of the governing parameters.

Figures 3–5 illustrate the effect of the suction parameter $S > 0$ on the velocity, temperature, and concentration profiles, respectively. The imposition of wall fluid suction for this problem has the effect of reducing the thicknesses of the thermal and concentration boundary layers, leading to an increase in the fluid velocity and a de-

TABLE 1

Values of the Free Parameters of the Analytical Solution

f_w	h_f	h_θ	h_φ	γ	M
1	−0.4	−1.5	−1.5	1.2	60
0	−0.4	−1.5	−1.0	1.1	60
−1	−0.5	−1.5	−0.6	0.7	80
1	−0.3	−1.5	−1.0	1.2	80
−1	−0.6	−0.8	−0.6	1.0	100

TABLE 2

Values of $f'(\eta)$ Obtained for Approximations of Various Orders of the Analytical Solution and by Numerical Calculations

η	Analytical solution							Results of numerical calculations
	$M = 10$	$M = 20$	$M = 40$	$M = 50$	$M = 60$	$M = 80$	$M = 100$	
0	0	0	0	0	0	0	0	0
0.1	0.6487	0.6484	0.6481	0.6482	0.6479	0.6478	0.6479	0.6481
0.2	0.8828	0.8828	0.8829	0.8827	0.8825	0.8825	0.8826	0.8827
0.3	0.9646	0.9644	0.9644	0.9642	0.9641	0.9641	0.9641	0.9643
0.4	0.9911	0.9612	0.9611	0.9611	0.9609	0.9608	0.9608	0.9610
1.0	0.9998	0.9998	0.9997	0.9997	0.9997	0.9997	0.9997	0.9998
2.0	0.9999	0.9999	0.9999	0.9999	0.9999	0.9999	0.9999	0.9999
3.0	0.9999	0.9999	0.9999	0.9999	0.9999	0.9999	0.9999	0.9999

TABLE 3

Values of $\theta(\eta)$ Obtained for Approximations of Various Orders of the Analytical Solution and by Numerical Calculation

η	Analytical solution							Results of numerical calculations
	$M = 10$	$M = 20$	$M = 40$	$M = 50$	$M = 60$	$M = 80$	$M = 100$	
0	1.0000	1.0000	1.0000	1.0000	1.0000	1.0000	1.0000	1.0000
0.1	0.5116	0.5116	0.5114	0.5108	0.5107	0.5107	0.5110	0.5110
0.2	0.2597	0.2596	0.2595	0.2594	0.2595	0.2595	0.2597	0.2597
0.3	0.1316	0.1315	0.1314	0.1309	0.1310	0.1310	0.1312	0.1312
0.5	0.0323	0.0324	0.0321	0.0321	0.0320	0.0321	0.0323	0.0323
1.0	0.0006	0.0006	0.0005	0.0005	0.0005	0.0005	0.0005	0.0005
2.0	0.0002	0	0	0	0	0	0	0
3.0	0.0001	0	0	0	0	0	0	0

TABLE 4

Values of $\varphi(\eta)$ Obtained for Approximations of Various Orders of the Analytical Solution and by Numerical Calculations

η	Analytical solution							Results of numerical calculations
	$M = 10$	$M = 20$	$M = 40$	$M = 50$	$M = 60$	$M = 80$	$M = 100$	
0	1.0000	1.0000	1.0000	1.0000	1.0000	1.0000	1.0000	1.0000
0.1	0.5272	0.5272	0.5271	0.5270	0.5267	0.5267	0.5267	0.5267
0.2	0.2753	0.2753	0.2752	0.2752	0.2750	0.2750	0.2750	0.2750
0.3	0.1450	0.1452	0.1451	0.1451	0.1451	0.1451	0.1451	0.1451
0.4	0.0743	0.0742	0.0741	0.0741	0.0741	0.0741	0.0741	0.0742
1.0	0.0010	0.0011	0.0010	0.0009	0.0008	0.0008	0.0008	0.0007
2.0	0.0002	0.0001	0	0	0	0	0	0
3.0	0.0001	0.0001	0	0	0	0	0	0

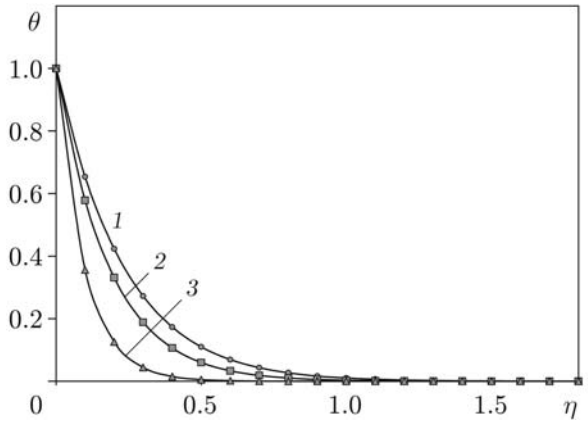

Fig. 4

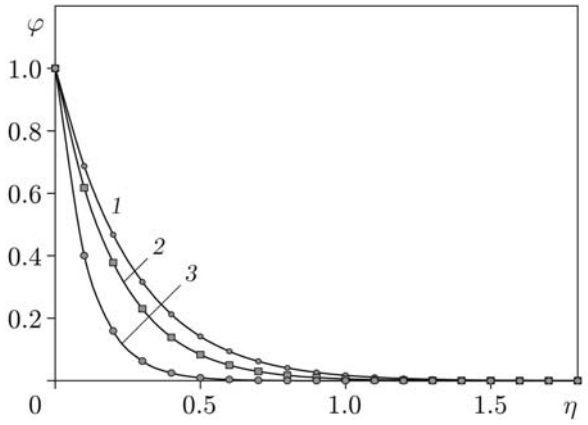

Fig. 5

Fig. 4. Temperature versus variable η for $\mathrm{Re}_x = 3$, $\mathrm{Re}_k = \mathrm{Gr} = \mathrm{Fn} = M_* = N = 1$, $\mathrm{Sc} = 0.62$, $\mathrm{Pr} = 0.73$, $\gamma = 1$, $M = 80$, $\tau = 1$, and various values of the parameter S (notation the same as in Fig. 3).

Fig. 5. Concentration versus variable η for $\mathrm{Re}_x = 3$, $\mathrm{Re}_k = \mathrm{Gr} = \mathrm{Fn} = M_* = N = 1$, $\mathrm{Sc} = 0.62$, $\mathrm{Pr} = 0.73$, $\gamma = 1$, $M = 80$, $\tau = 1$, and various values of the parameter S (notation the same as in Fig. 3)

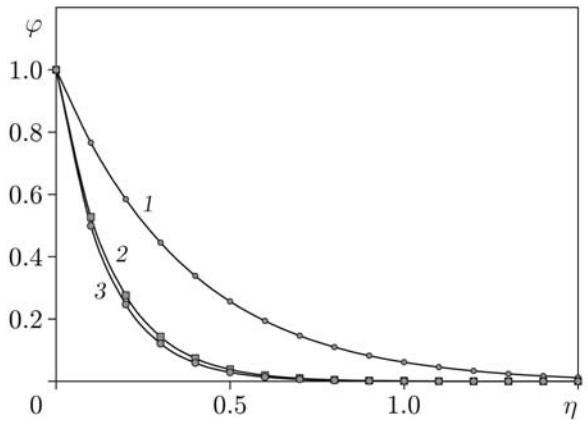

Fig. 6

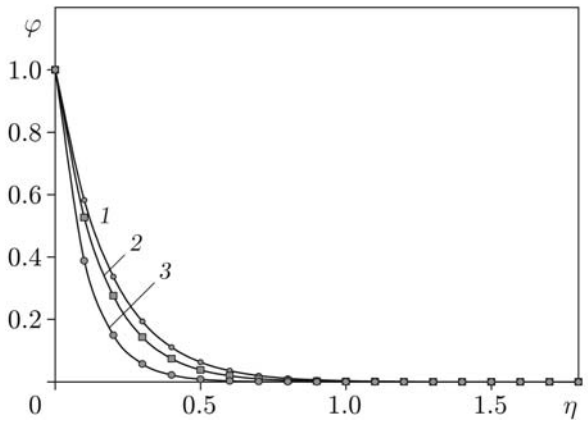

Fig. 7

Fig. 6. Concentration versus variable η for $\mathrm{Re}_x = 3$, $\mathrm{Re}_k = \mathrm{Gr} = \mathrm{Fn} = M_* = N = 1$, $S = 1$, $\mathrm{Pr} = 0.73$, $\gamma = 1$, $M = 80$, $\tau = 1$, and various values of Sc: 1) $\mathrm{Sc} = 0.22$ (hydrogen); 2) $\mathrm{Sc} = 0.62$ (water vapor); 3) $\mathrm{Sc} = 0.78$ (ammonia); points refer to numerical calculation results and curves to the analytical solution.

Fig. 7. Concentration versus variable η for $\mathrm{Re}_x = 3$, $\mathrm{Re}_k = \mathrm{Gr} = \mathrm{Fn} = M_* = N = 1$, $\mathrm{Sc} = 0.62$, $\mathrm{Pr} = 0.73$, $\gamma = 1$, $M = 80$, $S = 1$, and $\tau = 0.1$ (1), 1 (2), and 2 (3); points refer to numerical calculation results and curves to the analytical solution.

crease in its temperature and concentration. However, the imposition of wall fluid injection has the opposite effect, namely, decreases the fluid velocity and increases its temperature and concentration. The change in the thickness of the concentration layer is caused by two effects: 1) direct action of suction, leading to a decrease in the thickness of the concentration boundary layer; 2) indirect action of suction, leading to a decrease in the thickness of the thermal boundary layer, resulting in a higher temperature gradient and, hence, an increase in the thermophoretic force.

The effect of the Schmidt number on the concentration profile is shown in Fig. 6. It is seen that the concentration of the fluid decreases with increasing Schmidt number. The effect of the concentration buoyancy leads to an insignificant decrease in the fluid velocity.

The effect of the thermophoretic parameter τ on the concentration field is shown in Fig. 7. It is seen that fluid concentration decreases with increasing thermophoretic parameter. In particular, the effect of increasing the

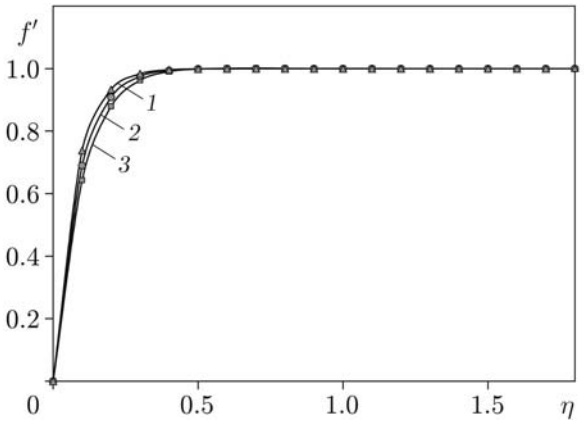

Fig. 8. Velocity versus variable η for $\mathrm{Re}_x = 3$, $\mathrm{Re}_k = \mathrm{Gr} = \mathrm{Fn} = N = 1$, $\mathrm{Sc} = 0.62$, $\mathrm{Pr} = 0.73$, $\gamma = 1$, $M = 80$, $S = 1$, $\tau = 1$, and $M_* = 0.5$ (1), 1 (2), and 3 (3); points refer to numerical calculation results and curves to the analytical solution.

thermophoretic parameter τ is limited by a decrease in the concentration with a slight increase in the slope of the concentration profiles at the wall. This is true only for small Schmidt numbers, for which the Brownian diffusion effect is large compared to the convection effect. However, for large Schmidt number ($\mathrm{Sc} > 100$) the diffusion effect is minimal compared to the convection effect and, therefore, the thermophoretic parameter τ is expected to alter the concentration boundary layer significantly. This is consistent with the data of Goren [1] on the thermophoresis of aerosol particles in a flat plate boundary layer.

Figure 8 presents typical velocity profiles for various values of the magnetic parameter. The effect of the transverse magnetic field on the electrically conducting fluid gives rise to a resistance type force called the Lorentz force, which slows down the fluid motion and leads to a decrease in the temperature and concentration.

Conclusions. Using the homotopy analysis method, we obtained an explicit, totally analytic, uniformly valid solution of the system of three fully coupled, highly nonlinear similarity equations describing heat and mass transfer by mixed convection in a porous medium. The validity of the analytical solution was verified by numerical results. To the best of authors knowledge, such kind of analytical solution has never been reported. In the mixed convection regime, thermophoretic particle deposition in the presence of a magnetic field has a substantial effect on the flow field and, thus, on the heat and mass transfer rate from the plate to the fluid. This explicit analytical solution might find wide application in engineering.

REFERENCES

1. S. L. Goren, "Thermophoresis of aerosol particles in laminar boundary layer on flat plate," *J. Colloid Interface Sci.*, **61**, 77–85 (1977).
2. W. G. England and A. F. Emery, "Thermal radiation effects on laminar free convection boundary layer of an absorbing gas," *J. Heat Transfer*, **31**, 37–44 (1969).
3. A. Raptis, "Flow of a micro polar fluid past a continuously moving plate by the presence of radiation," *Int. J. Heat Mass Transfer*, **4**, 2865–2866 (1988).
4. I. U. Mbeledogu and A. Ogulu, "Heat and mass transfer of an unsteady MHD natural convection flow of a rotating fluid past a vertical porous flat plate in the presence of radiative heat transfer," *Int. J. Heat Mass Transfer*, **50**, 1902–1908 (2007).
5. M. S. Alam, M. M. Rahman, and M. A. Sattar, "Effects of variable suction and thermophoresis on steady MHD combined free-forced convective heat and mass transfer flow over a semi-infinite permeable inclined plate in the presence of thermal radiation," *Int. J. Thermal Sci.*, **47**, 758–765 (2008).
6. M. A. Hossain and H. S. Takhar, "Radiation effects on mixed convection along a vertical plate with uniform surface temperature," *J. Heat Mass Transfer*, **31**, 243–248 (1996).

7. H. M. Duwairi and R. A. Damesh, "Magnetohydrodynamic natural convection heat transfer from radiate vertical porous surface," *J. Heat Mass Transfer*, **40**, 787–792 (2004).
8. H. M. Duwairi and R. A. Damesh, "MHD boundary aiding and opposing flows with viscous dissipation effects from radiate vertical surfaces," *Canad. J. Chem. Eng.*, **82**, 1–6 (2004).
9. H. M. Duwairi, "Viscous and joule heating effects on forced convection flow from radiate isothermal porous surfaces," *Int. J. Numer. Methods Heat Fluid Flow.*, **15**, 429–440 (2005).
10. R. A. Damesh, H. M. Duwairi, and M. Al-Odat, "Similarity analysis of magnetic field and thermal radiation effects on forced convection flow," *Turkish J. Eng. Env. Sci.*, **30**, 83–89 (2006).
11. P. Goldsmith and F. G. May, "Diffusiophoresis and thermophoresis in water vapour systems," in: C. N. Davies (ed.), *Aerosol Science*, Academic Press, London (1966), pp. 163–194.
12. S. Jayaraj, K. K. Dinesh, and K. L. Pallai, "Thermophoresis in natural convection with variable properties," *J. Heat Mass Transfer*, **34**, 469–475 (1999).
13. A. Selim, M. A. Hossain, and D. A. S. Rees, "The effect of surface mass transfer on mixed convection flow past a heated vertical flat permeable plate with thermophoresis," *Int. J. Thermal Sci.*, **42**, 973–982 (2003).
14. J. M. Hales, L. C. Schwendiman, and T. W. Horst, "Aerosol transport in a naturally-convected boundary layer," *Int. J. Heat Mass Transfer*, **15**, 1837–1849 (1972).
15. Ali J. Chamkha and I. Pop, "Effects of thermophoretic particle deposition in free convection boundary layer from a vertical flat plate embedded in a porous medium," *Int. Comm. Heat Mass Transfer*, **31**, 421–430 (2004).
16. D. A. Nield and A. Bejan, *Convection in Porous Media*, Springer, New York (1998).
17. P. V. S. N. Murthy and P. Singh, "Heat and mass transfer by natural convection in a non-Darcy porous medium," *Acta Mech.*, **38**, 243–254 (1999).
18. S. J. Liao, "The proposed homotopy analysis techniques for the solution of nonlinear problems, " Ph. D. Dissertation, Shanghai (1992).
19. S. J. Liao, "An approximate solution technique which does not depend upon small parameters: a special example," *Int. J. Nonlinear Mech.*, **30**, 371–380 (1995).
20. S. J. Liao "A uniformly valid analytical solution of two dimensional viscous flow over a semi-infinite flat plate," *J. Fluid Mech.*, **385**, 101–128 (1999).
21. S. J. Liao, "An explicit, totally analytic approximate solution for Blasius-viscous flow problems," *Int. J. Nonlinear Mech.*, **34**, 759–778 (1999).
22. S. J. Liao, "An analytic approximation of the drag coefficient for the viscous flow past a sphere," *Int. J. Nonlinear Mech.*, **37**, 1–18 (2002).
23. S. J. Liao and A. Campo, "Analytical solutions of the temperature distribution in Blasius viscous flow problems," *J. Fluid Mech.*, **453**, 411–425 (2002).
24. N. G. Kafoussias and N. D. Nanousis, "Magnetohydrodynamic laminar boundary layer flow over a wedge with suction or injection," *Canad. J. Phys.*, **75**, 733–741 (1997).
25. S. Gill, "A process for the step-by-step integration of differential equations in an automatic digital computing machine," *Math. Proc. Cambridge Philos. Soc.*, **47**, No. 1. 96–108 (1951).